M-2566

*J. Chem. Thermodynamics* **1991,** 23, 77–93

# Heat capacity and thermodynamic properties of synthetic heazlewoodite, $Ni_3S_2$, and of the high-temperature phase $Ni_{3\pm x}S_2$

SVEIN STØLEN, FREDRIK GRØNVOLD,

*Department of Chemistry, University of Oslo, 0315 Oslo 3, Blindern, Norway*

EDGAR F. WESTRUM, JR.,

*Department of Chemistry, University of Michigan, Ann Arbor, MI 48109, U.S.A.*

and GERMAN R. KOLONIN

*Institute of Geology & Geophysics, Siberian Branch of the USSR Academy of Sciences, 630090, Novosibirsk 90, U.S.S.R.*

*(Received 13 September 1990)*

The heat capacity of synthetic heazlewoodite ($Ni_3S_2$) was measured over the temperature range 5 K to 350 K by equilibrium adiabatic calorimetry and compared with earlier results. High-temperature results on this phase and on (two-phase) $Ni_{2.9}S_2$ were obtained through the transition regions and up to about 1000 K. In addition to comparing the post-(834 K)-transitional heat capacity with that of fast ionic conductors it is discussed phenomenologically with Helmholtz-energy modelling for the phase transformation. Thermodynamic functions have been evaluated and selected values are, for $R = 8.3144\ J \cdot K^{-1} \cdot mol^{-1}$:

| | $C_{p,m}/R$ | $\Delta_0^T S_m^\circ/R$ | $\Phi_m^\circ/R$ | $T$/K |
|---|---|---|---|---|
| (1/5)$Ni_3S_2$ | 2.844 | 3.204 | 1.469 | 298.15 |
| | 4.614 | 9.033 | 4.609 | 1000 |
| | $C_{p,m}/R$ | $\Delta_{298.15\,K}^T S_m^\circ/R$ | $\Delta_{298.15\,K}^T H_m^\circ/R$ | $T$/K |
| (1/4.9)$Ni_{2.9}S_2$ | 2.836 | 0 | 0 | 298.15 |
| | 4.667 | 5.613 | 3704.4 | 980 |

## 1. Introduction

The nickel sulfide $Ni_3S_2$ was first described by Petterd[1] and named heazlewoodite after the locality of its discovery. It was later synthesized by Alsén[2] who indicated the structure to be cubic on the basis of X-ray-diffraction results. Westgren[3] solved the structure of heazlewoodite, proposing the space group $R32$ with lattice constants $a = 408.0$ pm and $\alpha = 0.502 \cdot \pi$ as redetermined with corrections by Peacock.[4] The

0021–9614/91/010077+17 $02.00/0

sulfur atoms are in an approximately cubic body-centred arrangement and surrounded equidistantly by 9 nickel atoms at the corners of an irregular poyhedron. A recent neutron-diffraction investigation by Fjellvåg and Andersen[5] confirmed the structure and also delineated the temperature dependence of the lattice parameters. According to Kullerud and Yund,[6] the solubility of nickel or sulfur in heazlewoodite is less than 0.3 mass per cent near 800 K. More sensitive measurements by Rau[7] showed, however, that heazlewoodite has a measurable, although small, homogeneity range situated on the sulfur-rich side of $Ni_3S_2$. The decomposition temperature of the compound was reported to be $(838 \pm 5)$ K by Rau,[7] 826 K by Conard *et al.*,[8] 823 K by Sokolova,[9] and $(834 \pm 1)$ K by Ferrante and Gokcen.[10] Above this temperature a grossly non-stoichiometric $Ni_{3\pm x}S_2$ phase is present. On each side of the stoichiometric composition eutectoids are formed. The eutectoid temperatures are 806 K and 797 K on the nickel and sulfur-rich sides, respectively.[11] The homogeneity range of the high-temperature phase is known through early activity studies by Schenck and van der Forst,[12] and by Rosenqvist,[13] as well as through more precise and recent studies by Rau[7] and by Lin *et al.*[11] According to Lin *et al.* the phase field is divided by a two-phase region near mole fraction 0.41 of S.

The structure of the high-temperatue phase $Ni_{3\pm x}S_2$ is not well known. Crystallographic investigations were initiated by Kullerud and Yund.[6] They noted that changes in the composition of the highly non-stoichiometric phase are accompanied by pronounced changes in the relative intensities of the observed reflections, and by decreasing unit-cell dimensions with increasing nickel deficiency. The reflections obtained were, however, diffuse and the crystal symmetry was uncertain. Liné and Huber[14] first proposed a face-centered cubic cell, an interpretation later confirmed by Lamprecht and Manus[15] and by Fjellvåg and Andersen.[5] No sign of the proposed two-phase region in the high-temperature phase has been reported. On the contrary, the X-ray results at 923 K[5,14] give evidence of a smooth continuous variation in the lattice constant as a function of composition. The region of the constant sulfur activity, upon which the proposal of a two-phase region was made[11] was, however, not investigated in detail. It has been proposed[16] that by analogy with the notation of the high-digenite phase, as $Cu_{2-x}S$, the correct notation for the defect structure of $Ni_{3\pm x}S_2$ should be $Ni_{2-x}S$.

Heat-capacity results for $Ni_3S_2$ have been reported by Weller and Kelley[17] over the temperature range 55 K to 300 K, and the standard entropy at 298.15 K has been derived. More recently, drop calorimetry has been carried out by Conard *et al.*[8] and by Ferrante and Gokcen[10] over the temperature range 298 K to 1250 K. In addition, the enthalpy increment from 298 K to 873 K can be evaluated from results of Cemic and Kleppa.[18] Recent experimental determinations of formation energies are reported by them, by Mehrotha *et al.*,[19] and by Schaefer.[20] The thermodynamic properties of the binary system have been assessed by Lin *et al.*[11] and more recently by Sharma and Chang.[21]

In this first of a series of papers on the thermodynamic properties of nickel sulfides, the heat capacity of synthetic heazlewoodite, $Ni_3S_2$, and its cubic face-centred high-temperature modification, $Ni_{3\pm x}S_2$, are reported. High-temperature

results are also recorded for $Ni_{2.9}S_2$ which is a two-phase sample consisting of $Ni_3S_2$ and $Ni_7S_6$ at room temperature. This sample was chosen so that thermal effects related to the reported two-phase region of the high-temperature phase might be detected. Intermittently energized adiabatic calorimetry, which allows long equilibration periods, is a very sensitive technique for such a purpose. In addition, the post-transitional heat capacity is measured and discussed phenomenologically, using a Helmholtz-energy modelling for the phase transformation. The results of the calculations can also be compared with the transitional heat capacity of fast ionic conductors. Thermodynamic properties are evaluated and compared with previous results.

## 2. Experimental

### SYNTHESIS AND STRUCTURAL CHARACTERIZATION

$Ni_3S_2$ was prepared directly from the elements: nickel as 5 mm diameter rods >99.998 mass per cent pure and sulfur as 99.9999 mass per cent pure crystals from Koch-Light Laboratories, Colnbrook, England. Stoichiometric amounts of the elements were heated in an evacuated and sealed vitreous silica tube, constricted at the middle by a smaller diameter tube. Nickel was placed in one part of the tube, sulfur in the other, and the tube was put into a reclining tube furnace with the sulfur-containing compartment protruding. The nickel was heated to 870 K and the sulfur was allowed to melt and react with nickel in the hotter part of the tube. When most of the sulfur had combined with the nickel (2 d), a heating pad was wound around the exterior end of the vitreous silica tube so that the remaining sulfur was brought into reaction. This was accomplished overnight. The empty half of the silica tube was sealed off and discarded before the sample was equilibrated at 1270 K for 3 h. The sample was then finely crushed and transferred to the calorimetric ampoule.

$Ni_{2.9}S_2$ was prepared from the $Ni_3S_2$ sample by addition of sulfur. The mixture was heated slowly to 710 K in a vitreous silica tube and kept at this temperature for 12 h. The temperature was then raised to 1120 K. After 3 h the temperature was lowered to 770 K. The sample was kept at this temperature for 7 d and cooled with the furnace.

X-ray powder photographs of $Ni_3S_2$ and $Ni_{2.9}S_2$ were taken in Guinier-type cameras of 8.0 cm diameter. Cu ($K\alpha_1$) radiation was used with Si as internal standard.[22] The lattice parameters of heazlewoodite in $Ni_3S_2$ and $Ni_{2.9}S_2$ are $a = (408.1 \pm 0.1)$ pm and $\alpha = (0.4969 \pm 0.0001) \cdot \pi$ and $a = (408.1 \pm 0.1)$ pm and $\alpha = (0.4970 \pm 0.0001) \cdot \pi$, respectively. This is in good agreement with the parameters obtained by Parise: $a = (407.18 \pm 0.06)$ pm and $\alpha = (0.49699 \pm 0.00005) \cdot \pi$,[23] and by Fleet: $a = (408.21 \pm 0.05)$ pm and $\alpha = (0.49708 \pm 0.00005) \cdot \pi$.[24] The diagram for $Ni_{2.9}S_2$ included in addition a number of weak diffraction lines, most of which could be indexed in accordance with those of $\alpha$–$Ni_7S_6$.[25]

### CALORIMETRIC TECHNIQUE

The cryogenic heat-capacity measurements at Ann Arbor were made in the Mark X adiabatic cryostat, which has been described previously.[26] The sample was

contained in a gold-plated copper calorimeter (laboratory designation W-139). The calorimeter had a mass of 13.21 g and internal volume of 23 $cm^3$. The temperature of the calorimeter was measured with a Leeds & Northrup platinum encapsulated resistance thermometer in an entrant well. The thermometer was calibrated by the U.S. National Bureau of Standards against IPTS-68 and was considered to reproduce the thermodynamic scale within 0.03 K from 5 K to 300 K. About 150.58 g of sample were put in the calorimeter. To facilitate rapid thermal equilibration, 2.53 kPa at 300 K of helium gas was introduced after evacuation. The calorimeter was then sealed, placed in the cryostat, and cooled. The heat capacity of the empty calorimeter represented 27 per cent of the total heat capacity at temperatures below 50 K and decreased from about 25 to 18 per cent at higher temperatures.

The high-temperature calorimetric apparatus and measuring technique at Oslo have been described in detail previously.[27] The computer-operated calorimeter was intermittently heated, and surrounded by electrically controlled adiabatic shields. The sample was enclosed in an evacuated vitreous silica tube of about 50 $cm^3$ volume, tightly fitted into the silver calorimeter. A central entrant well in the tube served for the heater and platinum resistance thermometer. The resistance thermometer was calibrated locally, at the ice, steam, tin, zinc, and antimony points. Temperatures were judged to correspond with IPTS-68 to within 0.05 K at 900 K and within 0.1 K above. The heat capacity of the empty calorimeter was determined in a separate series of experiments with a standard deviation of a single measurement from the smoothed heat-capacity curve of about 0.15 per cent. Corrections were applied for differences in mass of the silica containers. The masses of the samples used were about 138.7 g and 133.5 g for $Ni_3S_2$ and $Ni_{2.9}S_2$, respectively.

## 3. Results

### HEAT CAPACITIES

The experimental heat capacities for $Ni_3S_2$ and $Ni_{2.9}S_2$ are given in chronological order in table 1 and presented graphically in figures 1(a) and 1(b). The approximate temperature increments used in the determinations can usually be inferred from the adjacent mean temperatures in the table. In table 2 the heat capacities in the transitional region are given together with the enthalpy increments. The experimental heat capacities for the low- and high-temperature regions were fitted to polynomials in temperature by the method of least squares. In the lowest temperature region the heat capacity of $Ni_3S_2$ was fitted by assuming a linear $C_{p,m}/T$ against $T^2$ relation. It was extrapolated to $T = 0$, giving an electronic heat capacity constant equal to zero within experimental accuracy. The analysis is made difficult by two abnormally low heat-capacity values in the low-temperature range. The estimated standard deviation of a single heat-capacity measurement in the low-temperature region is about 1 per cent at 7 K, decreasing to 0.1 per cent over the range 30 K to 350 K. The results for $Ni_3S_2$ in the range 300 K to 780 K were joined with the low-temperature results over the region 249 K to 348 K with a common standard deviation of 0.21 per cent. A single result was omitted in the fitting process.

TABLE 1. Molar heat capacities of (1/5)$Ni_3S_2$ and (1/4.9)$Ni_{2.9}S_2$ ($R = 8.31441\ J \cdot K^{-1} \cdot mol^{-1}$)

| $T$/K | $C_{p,m}/R$ | $T$/K | $C_{p,m}/R$ | $T$/K | $C_{p,m}/R$ | $T$/K | $C_{p,m}/R$ | $T$/K | $C_{p,m}/R$ | $T$/K | $C_{p,m}/R$ |
|---|---|---|---|---|---|---|---|---|---|---|---|
| $M\{(1/5)Ni_3S_2\} = 48.040\ g \cdot mol^{-1}$ | | | | | | | | | | | |
| High-temperature results—University of Oslo | | | | | | | | | | | |
| Series I | | 416.77 | 3.136 | 541.78 | 3.328 | 669.13 | 3.514 | 860.45 | 4.564 | 995.71 | 4.614 |
| 300.44 | 2.864 | 427.21 | 3.152 | 552.30 | 3.342 | 679.91 | 3.548 | 870.53 | 4.569 | Series III | |
| 311.38 | 2.903 | 437.60 | 3.170 | 562.85 | 3.358 | Series II | | 880.74 | 4.573 | 781.12 | 3.753 |
| 322.15 | 2.931 | 447.96 | 3.188 | 573.40 | 3.366 | 715.45 | 3.600 | 891.04 | 4.542 | $\Delta H$ detn. B | |
| 332.79 | 2.956 | 458.33 | 3.205 | 583.93 | 3.383 | 726.27 | 3.619 | 901.47 | 4.550 | 843.02 | 4.590 |
| 343.43 | 2.982 | 468.70 | 3.225 | 594.49 | 3.398 | 737.10 | 3.645 | 911.83 | 4.546 | Series IV | |
| 353.97 | 3.007 | 479.09 | 3.237 | 605.06 | 3.416 | 747.94 | 3.665 | 922.98 | 4.548 | 639.18 | 3.454 |
| 364.45 | 3.031 | 489.49 | 3.250 | 615.66 | 3.431 | 758.85 | 3.683 | 935.04 | 4.562 | 649.86 | 3.473 |
| 374.91 | 3.055 | 499.91 | 3.269 | 626.30 | 3.466 | 769.74 | 3.731 | 946.94 | 4.537 | 660.54 | 3.489 |
| 385.37 | 3.075 | 510.34 | 3.286 | 636.97 | 3.458 | $\Delta H$ detn. A | | 959.07 | 4.562 | 671.21 | 3.500 |
| 395.83 | 3.096 | 520.81 | 3.300 | 647.66 | 3.476 | 840.40 | 4.592 | 971.24 | 4.584 | 681.88 | 3.519 |
| 406.30 | 3.116 | 531.28 | 3.314 | 658.38 | 3.496 | 850.47 | 4.603 | 983.45 | 4.579 | 692.38 | 3.526 |
| Low-temperature results—University of Michigan | | | | | | | | | | | |
| Series V | | 27.17 | 0.09441 | 69.30 | 0.8300 | 134.96 | 1.899 | 208.33 | 2.494 | 291.09 | 2.821 |
| 8.65 | 0.00417 | 29.69 | 0.1225 | 73.86 | 0.9202 | 141.18 | 1.972 | 215.01 | 2.525 | 298.33 | 2.840 |
| 10.60 | 0.00646 | 32.51 | 0.1581 | 77.80 | 0.9999 | 147.43 | 2.037 | 221.69 | 2.562 | 305.56 | 2.860 |
| 11.75 | 0.00811 | 35.38 | 0.1983 | 83.12 | 1.102 | 153.69 | 2.101 | 228.37 | 2.593 | 312.78 | 2.884 |
| 13.36 | 0.00497 | 38.36 | 0.2440 | 88.46 | 1.205 | 159.98 | 2.158 | 235.07 | 2.622 | 319.51 | 2.902 |
| 14.82 | 0.01094 | 41.44 | 0.2944 | 93.86 | 1.299 | 166.28 | 2.214 | 241.76 | 2.653 | 326.79 | 2.921 |
| 15.84 | 0.01828 | 44.58 | 0.3490 | 99.45 | 1.393 | 172.59 | 2.266 | 248.62 | 2.683 | 334.03 | 2.940 |
| 17.28 | 0.02363 | 47.78 | 0.4073 | 105.18 | 1.486 | 178.88 | 2.312 | 255.64 | 2.709 | 341.27 | 2.968 |
| 19.02 | 0.03175 | 51.40 | 0.4756 | 110.88 | 1.573 | 185.23 | 2.356 | 262.66 | 2.735 | 347.90 | 2.972 |
| 20.75 | 0.04161 | 55.43 | 0.5539 | 116.62 | 1.658 | 191.68 | 2.398 | 269.68 | 2.764 | | |
| 22.74 | 0.05508 | 59.81 | 0.6402 | 122.58 | 1.741 | 198.13 | 2.445 | 276.72 | 2.783 | | |
| 24.94 | 0.07323 | 64.52 | 0.7352 | 128.75 | 1.822 | 201.66 | 2.459 | 283.85 | 2.807 | | |
| $M\{(1/4.9)Ni_{2.9}S_2\} = 47.823\ g \cdot mol^{-1}$ | | | | | | | | | | | |
| High-temperature results—University of Oslo | | | | | | | | | | | |
| Series VI | | 401.01 | 3.067 | 514.64 | 3.270 | 628.99 | 3.476 | 743.35 | 3.858 | 907.47 | 4.694 |
| 301.46 | 2.841 | 411.41 | 3.090 | 525.00 | 3.295 | 639.43 | 3.501 | 753.84 | 3.934 | 917.88 | 4.658 |
| 310.84 | 2.869 | 421.78 | 3.107 | 535.27 | 3.383[a] | 649.86 | 3.525 | 763.40 | 4.746 | 928.30 | 4.656 |
| 320.10 | 2.884 | 432.15 | 3.115 | 545.49 | 3.345[a] | 660.44 | 3.575 | 772.96 | 3.999 | 939.50 | 4.646 |
| 329.30 | 2.908 | 442.50 | 3.132 | 555.84 | 3.330 | 671.00 | 3.644 | 783.39 | 4.014 | 951.51 | 4.651 |
| 338.48 | 2.925 | 452.81 | 3.152 | 566.30 | 3.348 | 681.32 | 4.412 | $\Delta H$ detn. C | | 963.61 | 4.659 |
| 348.43 | 2.950 | 463.11 | 3.166 | 576.76 | 3.366 | 690.94 | 4.054 | 856.69 | 4.754 | 975.77 | 4.667 |
| 359.07 | 2.973 | 473.37 | 3.191 | 587.22 | 3.384 | 701.21 | 3.744 | 866.70 | 4.730 | | |
| 369.62 | 2.997 | 483.69 | 3.208 | 597.67 | 3.404 | 711.73 | 3.768 | 876.77 | 4.711 | | |
| 380.12 | 3.019 | 494.00 | 3.229 | 608.12 | 3.431 | 722.27 | 3.795 | 886.95 | 4.694 | | |
| 390.59 | 3.043 | 504.32 | 3.249 | 618.55 | 3.453 | 732.81 | 3.810 | 897.20 | 4.692 | | |

[a] Not included in the curve-fitting procedure (trace of NiO, $Ni_3S_4$, or cristobalite?).

For $Ni_{2.9}S_2$ the standard deviation over the range 301 K to 671 K, excluding two measurements, was 0.16 per cent.

## THERMODYNAMIC PROPERTIES

The enthalpy and entropy were evaluated by integrating the heat-capacity polynomials in temperature and adding the transitional enthalpies and entropies, see

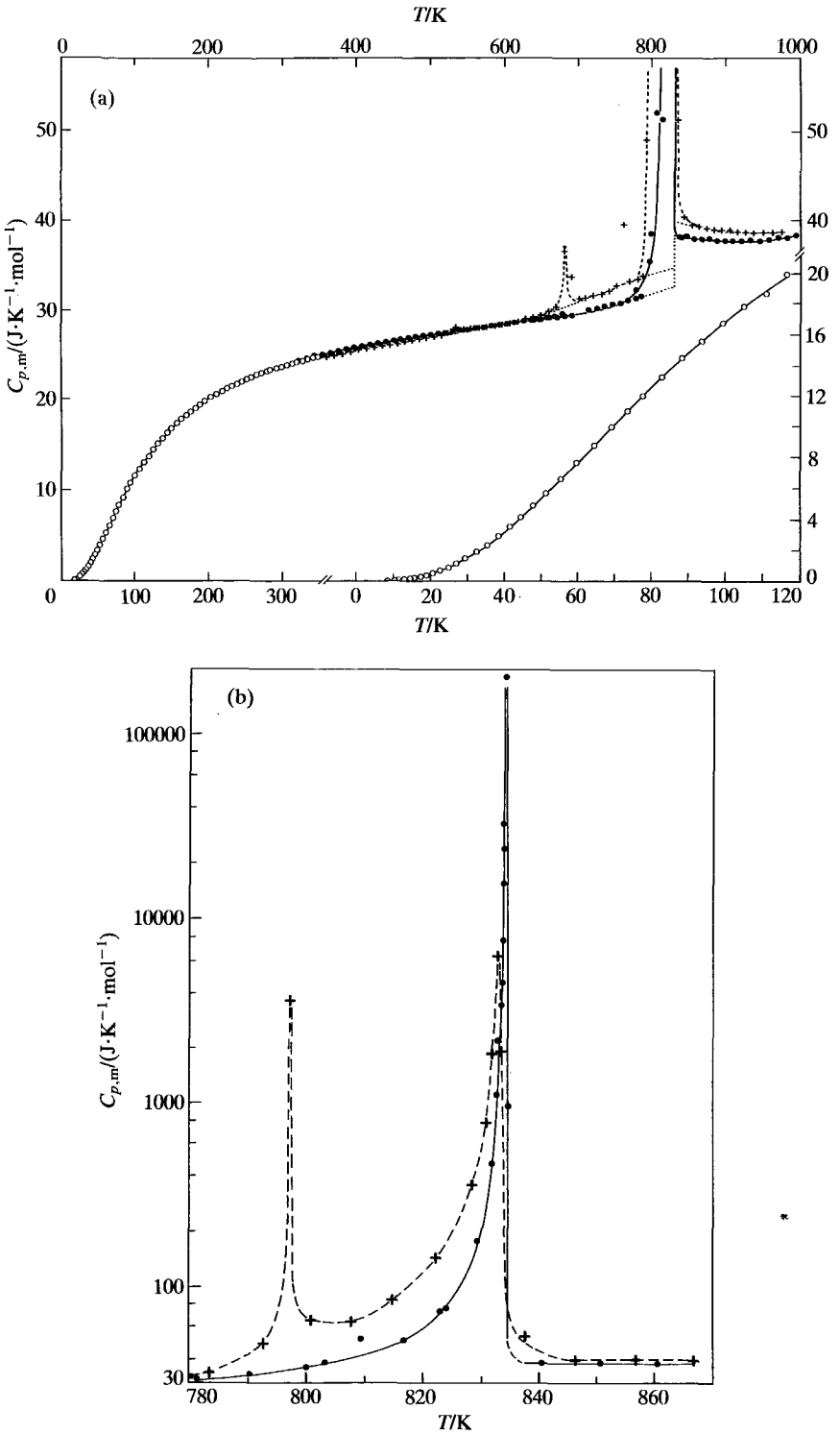


FIGURE 1. (a), Molar capacity of $(1/5)Ni_3S_2$; ○, results U of M; ●, results U of O; +, molar heat capacity of $(1/4.9)Ni_{2.9}S_2$, U of O. (b), Behavior in the region 780 K to 860 K; ●, $(1/5)Ni_3S_2$; +, $(1/4.9)Ni_{2.9}S_2$.

TABLE 2. Fractional molar enthalpy of transition for $(1/5)Ni_3S_2$ and $(1/4.9)Ni_{2.9}S_2$ ($R = 8.31441\ J \cdot K^{-1} \cdot mol^{-1}$)

| $\frac{T}{K}$ | $\frac{\Delta T}{K}$ | $\frac{C_{p,m}}{R}$ | $\frac{C_{p,m}(n.t.)}{R}$ | $\frac{t_{st}}{min}$ | $\frac{\Delta_{trs}H^\circ_m}{R \cdot K}$ | $\frac{T_{fin}}{K}$ |
|---|---|---|---|---|---|---|
| | | | $M\{(1/5)Ni_3S_2\} = 48.040\ g \cdot mol^{-1}$ | | | |
| $\Delta_{trs}H^\circ_m/(R \cdot K)$ detn. A | | | | | | |
| Series II, detns. 7 to 24 | | | | | | |
| 780.42 | 10.5038 | 3.863 | 3.753 | 61 | 1.2 | 785.674 |
| 790.73 | 10.0728 | 4.063 | 3.782 | 61 | 2.8 | 795.747 |
| 800.59 | 9.6851 | 4.271 | 3.811 | 61 | 4.5 | 805.432 |
| 809.19 | 7.5203 | 6.263 | 3.837 | 645 | 18.2 | 812.952 |
| 816.97 | 8.0347 | 6.178 | 3.862 | 61 | 18.6 | 820.987 |
| 824.26 | 6.5511 | 9.174 | 3.884 | 62 | 34.7 | 827.538 |
| 829.28 | 3.4925 | 20.94 | 3.897 | 60 | 59.5 | 831.030 |
| 831.77 | 1.4740 | 56.53 | 3.903 | 61 | 77.6 | 832.504 |
| 832.83 | 0.6413 | 135.8 | 3.905 | 87 | 84.6 | 833.143 |
| 833.30 | 0.3106 | 285.6 | 3.908 | 40 | 87.5 | 833.453 |
| 833.54 | 0.1654 | 540.3 | 3.908 | 40 | 88.7 | 833.619 |
| 833.67 | 0.09823 | 912.7 | 3.909 | 40 | 89.3 | 833.717 |
| 833.74 | 0.04817 | 1874 | 3.909 | 25 | 90.0 | 833.765 |
| 833.80 | 0.06304 | 2851 | 3.909 | 35 | 179.5 | 833.828 |
| 833.86 | 0.06779 | 3963 | 3.909 | 31 | 268.4 | 833.896 |
| 833.90 | 0.00368 | 24460 | 3.908 | 18 | 90.0 | 833.900 |
| 834.66 | 1.5164 | 114.1 | 4.606 | 51 | 166.0 | 835.416 |
| | | | | | 1361.1 | |
| $\Delta_{trs}H^\circ_m/(R \cdot K)$ detn. B | | | | | | |
| Series III, detns. 2 to 5 | | | | | | |
| 803.35 | 33.5712 | 4.638 | 3.807 | 80 | 27.9 | 820.139 |
| 823.61 | 6.9416 | 8.601 | 3.879 | 57 | 32.8 | 827.081 |
| 832.52 | 10.8762 | 122.2 | 4.169 | 65 | 1284.2 | 837.957 |
| | | | | | 1344.9 | |
| | | | $M\{1/4.9)Ni_{2.9}S_2\} = 47.823\ g \cdot mol^{-1}$ | | | |
| $\Delta_{trs}H^\circ_m/(R \cdot K)$ detn. C | | | | | | |
| Series VI, detns. 49 to 62 | | | | | | |
| 792.90 | 8.5922 | 5.886 | 4.118 | 50 | 15.2 | 797.187 |
| 797.30 | 0.21623 | 422.0 | 4.143 | 50 | 90.4 | 797.413 |
| 800.96 | 7.1032 | 7.972 | 4.165 | 40 | 27.0 | 804.516 |
| 808.16 | 7.2895 | 7.910 | 4.206 | 35 | 27.0 | 811.806 |
| 814.93 | 6.2395 | 10.12 | 4.245 | 35 | 36.7 | 818.045 |
| 822.26 | 8.4330 | 17.33 | 4.288 | 37 | 110.0 | 826.478 |
| 828.40 | 3.8446 | 44.01 | 4.324 | 37 | 152.6 | 830.323 |
| 830.79 | 0.93949 | 95.23 | 4.337 | 30 | 85.4 | 831.262 |
| 831.88 | 1.2348 | 223.6 | 4.343 | 40 | 270.7 | 832.497 |
| 832.67 | 0.34236 | 727.8 | 4.348 | 30 | 247.7 | 832.840 |
| 833.03 | 0.38264 | 239.9 | 4.617 | 37 | 90.0 | 833.222 |
| 837.53 | 8.6132 | 6.186 | 4.800 | 40 | 11.9 | 841.835 |
| 846.76 | 9.8580 | 4.871 | 4.777 | 40 | 0.9 | 851.693 |
| | | | | | 1165.5 | |

below. In the transitional region the heat capacity was read from large-scale plots and integrated manually. The thermodynamic values are given in table 3 at selected temperatures.

Low-temperature heat-capacity values for $Ni_3S_2$ by Weller and Kelley[17] deviate from those obtained here by +11 per cent at 50 K and by about −0.3 per cent in the

TABLE 3. Integral thermodynamic properties of $(1/5)Ni_3S_2$ and $(1/4.9)Ni_{2.9}S_2$ ($R = 8.31441\ J \cdot K^{-1} \cdot mol^{-1}$)

| $\frac{T}{K}$ | $\frac{C_{p,m}}{R}$ | $\frac{\Delta_0^T S_m^\circ}{R}$ | $\frac{\Delta_0^T H_m^\circ}{R \cdot K}$ | $\frac{\Phi_m^\circ}{R}$ | $\frac{T}{K}$ | $\frac{C_{p,m}}{R}$ | $\frac{\Delta_0^T S_m^\circ}{R}$ | $\frac{\Delta_0^T H_m^\circ}{R \cdot K}$ | $\frac{\Phi_m^\circ}{R}$ |
|---|---|---|---|---|---|---|---|---|---|
| | | | | $M\{(1/5)Ni_3S_2\} = 48.040\ g \cdot mol^{-1}$ | | | | | |
| | | | | Heazlewoodite | | | | | |
| 0 | 0 | 0 | 0 | 0 | 270 | 2.760 | 2.926 | 438.32 | 1.303 |
| 5 | 0.000 | 0.000 | 0.000 | 0.000 | 280 | 2.792 | 3.027 | 466.09 | 1.363 |
| 10 | 0.004 | 0.001 | 0.010 | 0.000 | 290 | 2.821 | 3.126 | 494.16 | 1.422 |
| 15 | 0.015 | 0.005 | 0.053 | 0.001 | 298.15 | 2.844 | 3.204 | 517.2 | 1.469 |
| 20 | 0.037 | 0.012 | 0.176 | 0.003 | 300 | 2.848 | 3.222 | 522.5 | 1.480 |
| 25 | 0.073 | 0.023 | 0.444 | 0.006 | 320 | 2.907 | 3.408 | 580.1 | 1.595 |
| 30 | 0.126 | 0.041 | 0.935 | 0.010 | 340 | 2.967 | 3.586 | 638.9 | 1.707 |
| 35 | 0.193 | 0.065 | 1.727 | 0.016 | 360 | 3.015 | 3.757 | 698.8 | 1.816 |
| 40 | 0.271 | 0.096 | 2.883 | 0.024 | 380 | 3.061 | 3.921 | 759.5 | 1.922 |
| 45 | 0.356 | 0.133 | 4.448 | 0.034 | 400 | 3.102 | 4.079 | 821.2 | 2.026 |
| 50 | 0.448 | 0.175 | 6.457 | 0.046 | 420 | 3.141 | 4.232 | 883.6 | 2.128 |
| 55 | 0.546 | 0.223 | 8.941 | 0.060 | 440 | 3.177 | 4.379 | 946.8 | 2.227 |
| 60 | 0.644 | 0.274 | 11.917 | 0.076 | 460 | 3.210 | 4.520 | 1010.7 | 2.323 |
| 70 | 0.845 | 0.389 | 19.357 | 0.112 | 480 | 3.241 | 4.658 | 1075.2 | 2.418 |
| 80 | 1.043 | 0.514 | 28.802 | 0.154 | 500 | 3.271 | 4.791 | 1140.3 | 2.510 |
| 90 | 1.230 | 0.648 | 40.174 | 0.202 | 520 | 3.299 | 4.919 | 1206.0 | 2.600 |
| 100 | 1.403 | 0.787 | 53.35 | 0.253 | 540 | 3.325 | 5.044 | 1272.2 | 2.689 |
| 110 | 1.562 | 0.928 | 68.18 | 0.308 | 560 | 3.352 | 5.166 | 1339.0 | 2.775 |
| 120 | 1.706 | 1.070 | 84.53 | 0.366 | 580 | 3.378 | 5.284 | 1406.3 | 2.859 |
| 130 | 1.838 | 1.212 | 102.26 | 0.425 | 600 | 3.405 | 5.399 | 1474.1 | 2.942 |
| 140 | 1.957 | 1.353 | 121.25 | 0.487 | 620 | 3.432 | 5.511 | 1542.5 | 3.023 |
| 150 | 2.064 | 1.491 | 141.36 | 0.549 | 640 | 3.461 | 5.620 | 1611.4 | 3.103 |
| 160 | 2.159 | 1.628 | 162.49 | 0.612 | 660 | 3.492 | 5.727 | 1681.0 | 3.181 |
| 170 | 2.245 | 1.761 | 184.52 | 0.676 | 680 | 3.526 | 5.832 | 1751.1 | 3.257 |
| 180 | 2.320 | 1.892 | 207.35 | 0.740 | 700 | 3.563 | 5.935 | 1822.0 | 3.332 |
| 190 | 2.388 | 2.019 | 230.90 | 0.804 | 720 | 3.603 | 6.036 | 1893.7 | 3.406 |
| 200 | 2.449 | 2.143 | 255.08 | 0.868 | 740 | 3.648 | 6.135 | 1966.2 | 3.478 |
| 210 | 2.504 | 2.264 | 279.85 | 0.931 | 760 | 3.697 | 6.233 | 2039.5 | 3.549 |
| 220 | 2.554 | 2.382 | 305.14 | 0.995 | 780 | 3.751 | 6.330 | 2113.9 | 3.620 |
| 230 | 2.602 | 2.496 | 330.93 | 1.057 | 800 | 3.810 | 6.425 | 2189.6 | 3.688 |
| 240 | 2.646 | 2.608 | 357.17 | 1.120 | 820 | 3.869 | 6.520 | 2266.5 | 3.756 |
| 250 | 2.687 | 2.717 | 383.33 | 1.181 | 833.90 | 3.909 | 6.585 | 2320.5 | 3.802 |
| 260 | 2.725 | 2.823 | 410.89 | 1.242 | | | | | |
| | | | | High-temperature phase | | | | | |
| 833.90 | 4.608 | 8.198 | 3665.3 | 3.802 | 920 | 4.546 | 8.652 | 4058.5 | 4.241 |
| 840 | 4.599 | 8.237 | 3693.4 | 3.840 | 940 | 4.551 | 8.749 | 4149.4 | 4.335 |
| 860 | 4.576 | 8.345 | 3785.1 | 3.944 | 960 | 4.563 | 8.845 | 4240.6 | 4.428 |
| 880 | 4.560 | 8.450 | 3876.5 | 4.045 | 980 | 4.585 | 8.940 | 4332.1 | 4.519 |
| 900 | 4.550 | 8.552 | 3967.6 | 4.144 | 1000 | 4.614 | 9.033 | 4424.0 | 4.609 |

TABLE 3—*continued*

| $\frac{T}{K}$ | $\frac{C_{p,m}}{R}$ | $\frac{\Delta_{298.15K}^{T} S_m^\circ}{R}$ | $\frac{\Delta_{298.15K}^{T} H_m^\circ}{R \cdot K}$ | $\frac{T}{K}$ | $\frac{C_{p,m}}{R}$ | $\frac{\Delta_{298.15K}^{T} S_m^\circ}{R}$ | $\frac{\Delta_{298.15K}^{T} H_m^\circ}{R \cdot K}$ |
|---|---|---|---|---|---|---|---|
| | | | $M\{(1/4.9)N_{2.9}S_2\} = 47.823\ g \cdot mol^{-1}$ | | | | |
| | | | $(Ni_3S_2 + Ni_7S_6)$ phases | | | | |
| 298.15 | 2.836 | 0 | 0 | 600 | 3.410 | 2.173 | 948.1 |
| 300 | 2.838 | 0.0175 | 5.249 | 620 | 3.449 | 2.286 | 1016.7 |
| 320 | 2.883 | 0.2024 | 62.46 | 640 | 3.502 | 2.396 | 1086.2 |
| 340 | 2.931 | 0.3784 | 120.6 | 660 | 3.578 | 2.505 | 1156.9 |
| 360 | 2.972 | 0.5476 | 179.7 | 680 | 3.636 | 2.612 | 1229.1 |
| 380 | 3.021 | 0.7095 | 239.7 | 685 | 3.651 | 2.639 | 1247.3 |
| 400 | 3.060 | 0.8655 | 300.6 | 685 | 3.651 | 2.661 | 1262.2 |
| 420 | 3.097 | 1.016 | 362.1 | 700 | 3.733 | 2.741 | 1317.6 |
| 440 | 3.132 | 1.161 | 424.4 | 720 | 3.777 | 2.846 | 1392.7 |
| 460 | 3.168 | 1.300 | 487.5 | 740 | 3.856 | 2.951 | 1469.0 |
| 480 | 3.203 | 1.436 | 551.1 | 760 | 3.947 | 3.055 | 1547.0 |
| 500 | 3.230 | 1.567 | 615.6 | 780 | 4.012 | 3.158 | 1626.5 |
| 520 | 3.275 | 1.696 | 680.7 | 800 | 4.160 | 3.261 | 1708.2 |
| 540 | 3.310 | 1.820 | 746.5 | 820 | 4.276 | 3.365 | 1792.6 |
| 560 | 3.344 | 1.941 | 813.0 | 833 | 4.350 | 3.433 | 1848.7 |
| 580 | 3.376 | 2.059 | 880.3 | | | | |
| | | | $Ni_{3+x}S_2$ | | | | |
| 833 | 4.818 | 4.850 | 3016.2 | 920 | 4.673 | 5.319 | 3425.0 |
| 840 | 4.797 | 4.890 | 3047.8 | 940 | 4.652 | 5.419 | 3518.3 |
| 860 | 4.742 | 5.002 | 3143.2 | 960 | 4.644 | 5.517 | 3611.3 |
| 880 | 4.699 | 5.110 | 3237.6 | 980 | 4.667 | 5.613 | 3704.4 |
| 900 | 4.685 | 5.216 | 3331.4 | | | | |

100 K to 300 K range. The standard entropy at 298.15 K is insignificantly different, although their extrapolation led to a value at 50 K that is 12 per cent higher.

The drop-calorimetric results by Ferrante and Gokcen[10] give about 1 per cent lower heat-capacity values than those obtained here in the ambient-temperature region, about −1.6 per cent at 500 K, and −0.7 per cent at 800 K. In the post-transitional region from 834 K to 900 K, the former results are about 0.7 per cent higher than the present ones. However, a steadily decreasing heat capacity was reported by Ferrante and Gokcen[10] also above 900 K, while the presently obtained results show a minimum around 920 K. Thus, we have found a 2.2 per cent higher heat capacity for $Ni_3S_2$ at 1000 K than that reported by Ferrante and Gokcen.[10] The enthalpy increment $\Delta_{298.15\,K}^{1000\,K} H_m^\circ$ is lower than ours by 0.6 per cent, and that by Conard *et al.*[8] is lower than ours by 1.0 per cent over the same region.

## 4. Discussion

$Ni_3S_2$

No major heat-capacity effects were observed for the low-temperature phase of $Ni_3S_2$, heazlewoodite, between 10 K and the decomposition temperature 834 K. A smooth regular increase was observed up to 760 K, where a more strongly increasing trend starts. This increase is probably connected with the observed change (see

Rau)[7] in the homogeneity range of heazlewoodite near its decomposition temperature.

The transformation of heazlewoodite into the high-temperature $\beta_1$-$Ni_{3\pm x}S_2$ phase occurs over a range in temperature. Two-thirds of the enthalpy increment is found within a 0.76 K interval around 833.67 K and 90 per cent is found within 4.4 K (see table 2, $\Delta_{trs}H^\circ_m$ determination A). The molar heat capacity rises to a maximum of $2 \cdot 10^5$ J·K$^{-1}$·mol$^{-1}$ during the transition, with a resulting enthalpy of transition for (1/5)$Ni_3S_2$ of 11317 J·mol$^{-1}$.

Determination B gives a 135 J·mol$^{-1}$ lower value, which is chosen here. It is based upon the observation that most of the difference arises in the 790 K to 820 K region where traces of nickel might react slowly. Furthermore, the long time required for reaching equilibrium in this temperature range (up to 645 min) also impairs the accuracy of determination A.

The transitional enthalpy obtained here agrees well with the earlier determinations by Conard *et al.*[8] and by Ferrante and Gokcen[10] and also with the evaluations by Mah and Pankratz[28] and Pankratz *et al.*,[29] see table 4. The transition temperature varies from 826 K to 840 K. In the assessment of the thermodynamic properties of the binary mixture by Lin *et al.*[11] the transitional enthalpy is about 7 per cent lower than the two newest experimental determinations, and is presumably in error.

The enthalpy and entropy of transition are surprisingly large, and exceed those observed for the fast-ionic-conductor transitions in $Ag_2S$,[30] $Cu_2S$,[31] and AgI,[32] (see table 5). In addition, the molar heat capacity in the post-transitional region is also large: $\approx$38 J·K$^{-1}$·mol$^{-1}$. The origin of these anomalous features is not known. The isobaric expansivity changes but little at the transition, being $4.7 \cdot 10^{-5}$ K$^{-1}$ below and $6 \cdot 10^{-5}$K$^{-1}$ above the transition temperature,[5] The dilational contribution will, hence, not be much larger for the high-temperature phase than for heazlewoodite, provided that the compressibilities of the two structures are comparable. The transition from heazlewoodite to the high-temperature structure involves a complete rearrangement of the crystallographic structure from a rhombohedral one at low temperature to a cubic high-temperature phase. The transition is, hence, much more complicated than pure order-disorder. Knowledge about the structures is limited. Although the low-melting highly non-stoichiometric $Ni_{3+x}S_2$ phase is very important, being the cause of rapid corrosion of Ni in a sulfur-containing atmosphere, the heazlewoodite structure is much more

TABLE 4. Transformation molar enthalpies and entropies for (1/5)$Ni_3S_2$ ($R = 8.31441$ J·K$^{-1}$·mol$^{-1}$)

| Authors | Ref. | Year | $T_{trs}$ | $\Delta_{trs}H^\circ_m/(R \cdot K)$ | $\Delta_{trs}S^\circ_m/R$ |
|---|---|---|---|---|---|
| Conard *et al.* | 8 | 1977 | 826 | 1343 | 1.626 |
| Mah & Pankratz | 28 | 1976 | 838 | 1346.5 | 1.612 |
| Lin *et al.* | 11 | 1978 | 838 | 1252.6 | 1.495 |
| Ferrante & Gokcen | 10 | 1982 | 834 | 1341 | 1.607 |
| Pankratz *et al.* | 29 | 1984 | 840 | 1346 | 1.602 |
| Present | | 1990 | 834 | 1344.9 | 1.613 |

TABLE 5. Transformation molar enthalpy and entropy values for some fast ionic conductors ($R = 8.31441\ J \cdot K^{-1} \cdot mol^{-1}$)

| Compound | Authors | Ref. | Year | $T_{trs}$ | $\Delta_{trs}H^{\circ}_m/(R \cdot K)$ | $\Delta_{trs}S^{\circ}_m/R$ |
|---|---|---|---|---|---|---|
| (1/3)$Ag_2S$ | Grønvold & Westrum | 30 | 1986 | 450 | 162.8 | 0.362 |
| (1/3)$Cu_2S$ | Grønvold & Westrum | 31 | 1987 | 376 | 462.7 | 1.231 |
| (1/2)AgI | Shaviv *et al.* | 32 | 1989 | 420 | 378.9 | 0.902 |
| (1/5)$Ni_3S_2$ | Present | | 1990 | 834 | 1344.9 | 1.613 |

precisely determined.[3,4] The complexity of the high-temperature structure, involving large anharmonic vibrations and/or changing defect structure, is indicated by the surprisingly bad agreement between the observed and calculated structure factors for all proposed crystallographic arrangements. For related sulfide phases, complex structural models have been proposed. $Cu_{2-x}S$ with a cubic face-centered structure has been proposed to have a complex cluster-type distribution of filled and empty planes of atoms. The model is based on imaging electron-diffraction studies.[33,34] More recently, a neutron-diffraction study of the high digenite ($Cu_{2-x}S$) structure by Oliviera *et al.*[35] has shown that the copper atom distribution is not as complex as previously supposed.[16,36,37] The copper atoms are distributed over the 32(f) positions in space group *Fm3m* about 50 pm away from the tetrahedral centers towards the faces of the tetrahedra with strongly anharmonic vibrations. For another highly non-stoichiometric transition metal sulfide, $Fe_{1-x}S$, the presence of an infinitely adaptive structure has been proposed by Anderson.[38]

$Ni_{2.9}S_2$

According to Lin *et al.*[11] the non-stoichiometric $Ni_{3\pm x}S_2$ phase is actually split in two by a two-phase region near mole fraction 0.41 of S, indicated in figure 2 as $\beta_1 + \beta_2$. This conclusion was based on the observed sulfur fugacities, while directly observed changes in the crystallographic structure remain to be reported. X-ray results by Fjellvåg and Andersen[5] indicate a smooth continuous variation in the lattice constant of the cubic structure as a function of composition. A large contraction in the unit cell is, however, observed. The volume of $Ni_{2.8}S_2$ is 10 per cent smaller than that of $Ni_{3.4}S_2$ at 923 K. In order to detect effects with origin in the reported two-phase region, the heat capacity of $Ni_{2.9}S_2$, chosen so as to obtain an optimal composition for the purpose, was determined at high temperatures. Consequently, the sample is a two-phase mixture of $Ni_3S_2$ and $Ni_7S_6$ at room temperature.

The small transition observed for $Ni_{2.9}S_2$ at 685 K is due to transformation of the nearly stoichiometric compound $Ni_7S_6$(or) into a non-stoichiometric high-temperature phase, here denoted as $Ni_7S_6$(t).[11] Compositional changes of this "new" phase give rise to high heat-capacity values, relative to heazlewoodite, below 797 K. Here peritectoid formation of the $\beta_2$-phase takes place with a transitional enthalpy of about $750\ J \cdot mol^{-1}$. From 797 K to 833 K the composition of the

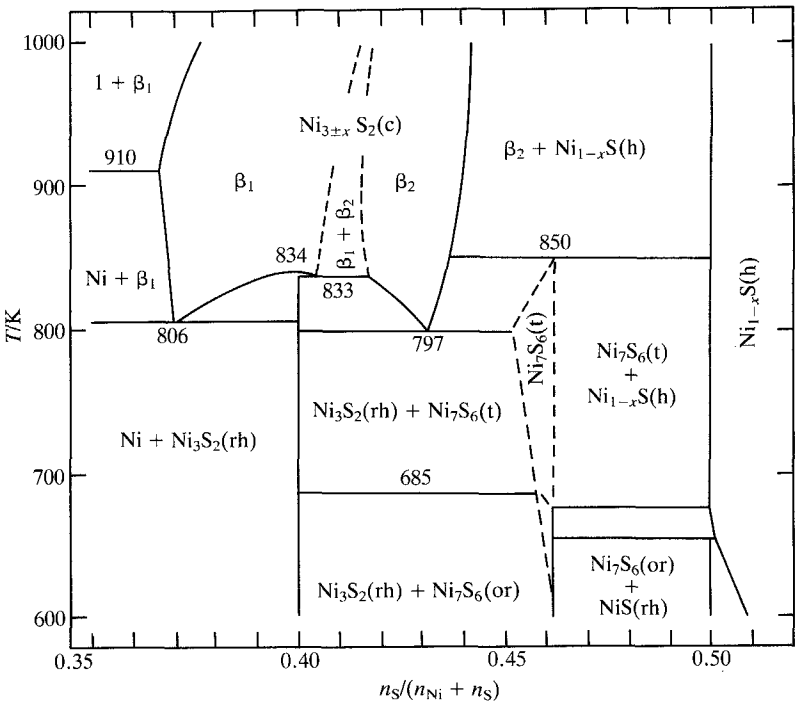


FIGURE 2. Phase relations of nickel sulfides in the range $Ni_2S$ to NiS. $Ni_3S_2$ rhombohedral represents synthetic heazlewoodite; $\beta_1$ and $\beta_2$ the nickel-rich and the sulfur-rich parts of the high-temperature $Ni_{3\pm x}S_2$ cubic phase. Other phases are Ni(s), a nickel-rich liquid l, the orthorhombic and tetragonal forms of $Ni_7S_6$, and the rhombohedral and hexagonal forms of NiS.

high-temperature phase changes continuously, giving molar heat capacities on the average (20 to 40) $J \cdot K^{-1} \cdot mol^{-1}$ larger than those observed for $Ni_3S_2$. Finally, at 833 K, $Ni_{2.9}S_2$ transforms to the high-temperature phase; see figures 1(b) and 2. The transition, with a maximum molar heat capacity of only $6 \cdot 10^3 J \cdot K^{-1} \cdot mol^{-1}$, is much more gradual than that observed in $Ni_3S_2$. The transition temperatures is 833 K for $Ni_{2.9}S_2$ and the obtained enthalpy and entropy of transition are 13 per cent lower than those observed for $Ni_3S_2$.

According to the phase diagram proposed by Lin *et al.*[11] a high-temperature tail should be observed on the heat-capacity peak. For $Ni_3S_2$, an abrupt decrease in the heat capacity is observed at the transition temperature, see figures 1 and 2, and an almost constant heat capacity is observed for the high-temperature phase. The size of the effect observed in $Ni_{2.9}S_2$ is, however, very small, indicating that any structural changes occurring must be minor. The two-phase region, hence, may represent merely a region of changing defect structure. No structural values are at hand. Different structural regimes within a homogeneity range have, however, been proposed for wüstite,[39] and also for the more sulfur-rich non-stoichiometric nickel sulfide, $Ni_{1-x}S$.[40] No definite conclusion, as to the existence of the reported two-phase region can, however, be drawn on the basis of the present heat capacities.

## PHENOMENOLOGY OF THE PHASE TRANSITION AND THE POST-TRANSITIONAL HEAT CAPACITY

The heat capacity of $Ni_{3\pm x}S_2$ is anomalously large and can possibly be connected with the changing disorder in the grossly non-stoichiometric phase. The large degree of disorder taking place during the solid-state transition is illustrated by the fact that the enthalpy of transition of heazlewoodite is much larger than the enthalpy of melting of $Ni_{3\pm x}S_2$. Although the high post-transitional heat capacity may be connected with the high mobility of the metal ions, this argument is weakened by the fact that the heat capacities in the fast-ionic-conductor phases of $Ag_2S$,[30] $Cu_2S$,[31] and AgI,[32] are much lower; see figure 3. A phenomenological interpretation of these observations can be given using a Helmholtz-energy model for the phase transition. Assuming the existence of a metastable low-temperature structure from which the high-temperature structure can be generated through formation of interstitial cations, the following molar Helmholtz energy can be formulated:[41]

$$A_m(x, T) = xU_m - \tfrac{1}{2}\lambda x^2 + RT\{x \cdot \ln x + (1-x) \cdot \ln(1-x) - x \cdot \ln g\},$$

where $U_m$ is the molar energy required to transfer a cation to an interstitial site and $\lambda$ is connected to the interaction of an interstitial cation and the strain field left behind at the vacancy,[42] $x$ is the fraction of interstitial cations, and $g$ is the degeneracy of the interstitial position relative to the ground-state position. Similar equations have been derived by a number of investigators,[43-45] in which the interpretation of $\lambda$ and

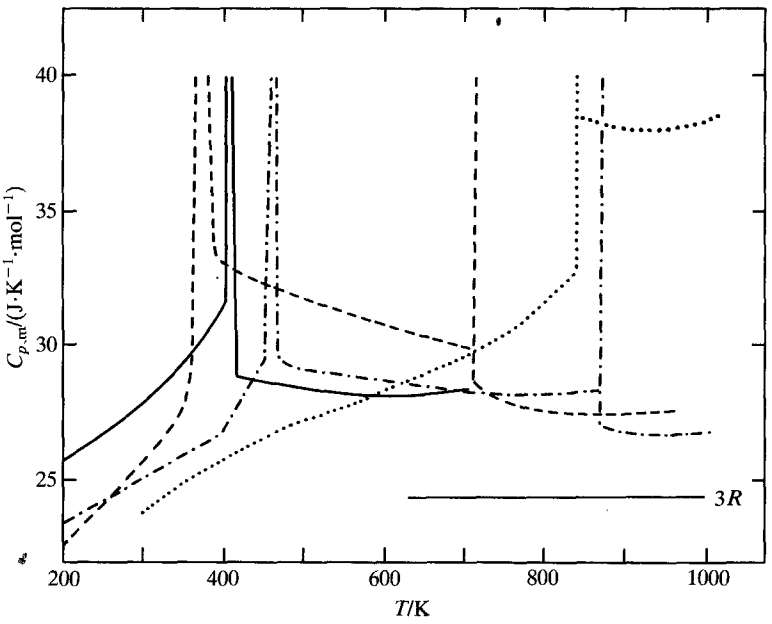


FIGURE 3. Molar heat capacities in transition regions for some fast ionic conductors and $Ni_3S_2$. —·—, (1/3)$Ag_2S$;[30] - - - -, (1/3)$Cu_2S$;[31] ——, (1/2)AgI,[32] and · · · ·, (1/5)$Ni_3S_2$.

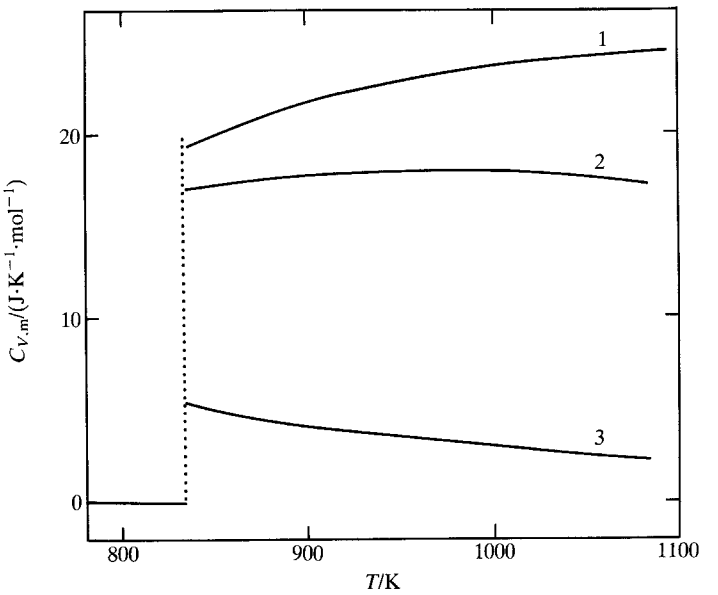


FIGURE 4. Molar heat-capacity contributions from interstitial cation-site occupancy change for different $\lambda/U_m$ ratios and degeneracies $g$ above $T_c = 834$ K. 1, $\lambda/U_m = 1.65$ and $g = 3$; 2, $\lambda/U_m = 1.60$ and $g = 3$; 3, $\lambda/U_m = 1.60$ and $g = 2$.

$g$ differ. Minimization of $A$ with respect to $x$ gives the equilibrium ratio of interstitials:

$$U_m - \lambda x = RT[\ln\{g(x^{-1}-1)\}].$$

First-order or continuous phase transitions result, depending on the ratio $\lambda/U_m$ and the degeneracy $g$. For more details, see Strässler and Kittel[41] and Rice *et al.*[42] The heat-capacity contribution from the order-disorder process is given by

$$C_{V,m,i} = T(d^2A_m/dx^2)(dx/dT)^2.$$

Hence,[43]

$$C_{V,m,i} = R^2T\{2RTx(1-x) - 2\lambda x^2(1-x)^2\} \times (\{\ln(1-x)\}^2x^{-1}[2U_m - 2RT\cdot\ln g - \lambda x - \lambda x(1-x)\cdot\ln\{(1-x)/x\}]^{-1})^2.$$

The condition for a first-order transition is[41]

$$\lambda/U_m > [2\{1+(\ln g)/2\}^{-1}],$$

and the transition temperature is given by

$$RT_{trs} = (U_m - \lambda/2)/\ln g.$$

Using these equations the heat-capacity contribution was calculated for different $\lambda/U_m$ ratios and $g$ values, in order to see whether the large observed heat capacities of $Ni_3S_2$ and $Cu_2S$ might be modelled. In figure 4 the results of calculations for

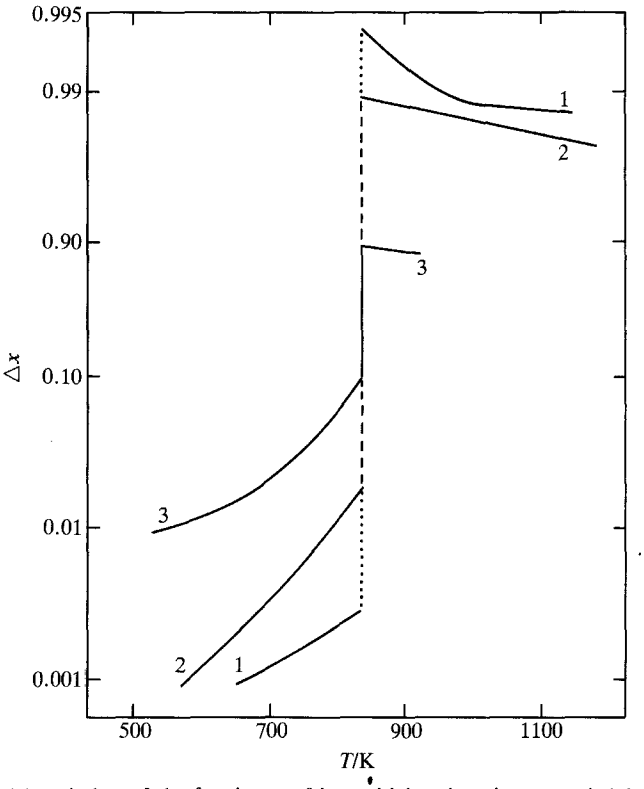


FIGURE 5. Model variation of the fraction $x$ of interstitial cation sites occupied for different $\lambda/U_m$ ratios and degeneracies $g$, for $T_c = 834$ K. 1, $\lambda/U_m = 1.65$ and $g = 3$; 2, $\lambda/U_m = 1.60$ and $g = 3$; 3, $\lambda/U_m = 1.60$ and $g = 2$.

$\lambda/U_m = 1.6$ with $g = 2$ and 3, and for $\lambda/U_m = 1.65$ and $g = 3$, are presented. They correspond to $U_m = (24.0, 38.1, \text{and } 43.5)\ \text{kJ} \cdot \text{mol}^{-1}$, respectively, $T_{trs}$ being 834 K. The three curves represent three different situations. $\lambda/U_m = 1.65$ with $g = 3$ corresponds to a large and regularly increasing heat-capacity increment over the temperature interval studied. It is comparable to that observed for $Ni_3S_2$, while the lack of downward curvature in the observed heat capacity probably arises from increased dilational contribution. $\lambda/U_m = 1.6$ with $g = 3$ gives a maximum in the heat capacity above the transition temperature, whereas reducing $g$ to 2 results in a much smaller and steadily decreasing heat capacity. Here a maximum in heat capacity occurs for $T < T_{trs}$, where the high-temperature structure is unstable. The magnitude of the contributions depends largely on the chosen $\lambda/U_m$ ratio and degeneracy. The large post-transitional heat capacity presently observed, and the lower and continuously decreasing heat capacity observed in the fast-ionic-conducting β-$Cu_2S$ phase[31] are, however, phenomenologically described using the same model for the Helmholtz energy.

In figure 5 the corresponding variations in the interstitial fraction are shown for

the three cases. The large discontinuity in $x$ and the slightly decreasing interstitial fraction in the post-transitional region should be noted. The discontinuity is largest for $\lambda/U_m = 1.65$ and $g = 3$, $\Delta x \approx 0.99$, and smallest for $\lambda/U_m = 1.6$ and $g = 2$, $\Delta x \approx 0.80$. Physically, the solutions represent transformations where the interstitial positions are filled discontinuously by very large fractions of the metal atoms, followed by a return of some of them to their previous positions. The solution, hence, rests on a somewhat surprising physical picture, which needs further confirmation. It does, however, explain the observed heat capacities.

The portion of this work done at the University of Michigan was supported by the Structural Chemistry and Chemical Thermodynamics Program, Division of Chemistry, National Science Foundation, whereas the work done at the University of Oslo was supported by the Norwegian Research Council for Science and the Humanities. The assistance of Bjørn Lyng Nielsen with the preparation of the samples and in the higher-temperature calorimetric measurements is gratefully acknowledged.

## REFERENCES

1. Petterd, W. F. *Catalogue of the Minerals in Tasmania.* Launceston, **1889,** p. 47.
2. Alsén, N. *Geol. Föreningen Stockholm Förhandl.* **1925,** 47, 19.
3. Westgren, A. *Z. anorg. allg. Chem.* **1938,** 239, 82.
4. Peacock, M. A. *Am. Mineral.* **1947,** 32, 484; *Univ. Toronto Studies Geol. Series* **1947,** 51, 59.
5. Fjellvåg, H.; Andersen, A. Unpublished results.
6. Kullerud, G.; Yund, R. A. *J. Petrology* **1962,** 3, 126.
7. Rau, H. *J. Phys. Chem. Solids* **1976,** 37, 929.
8. Conard, B. R.; Sridhar, R.; Warner, J. S. 106th AIME annual meeting, Atlanta, Georgia, U.S.A., **1977.**
9. Sokolova, M. A. *Zhur. Neorg. Khim.* **1956,** 1, 1440.
10. Ferrante, M. J.; Gokcen, N. A. *U.S. Bureau of Mines Rept. Inv. 8745,* **1982.**
11. Lin, R. Y.; Hu, D. C.; Chang, Y. A. *Met. Trans.* **1978,** 9B, 531.
12. Schenck, R. von; Forst, P. van der *Z. anorg. allg. Chem.* **1939,** 241, 145.
13. Rosenqvist, T. *J. Iron Steel Inst.* **1954,** 176, 34.
14. Liné, G.; Huber, M. *C.R. Acad. Sci. Paris* **1963,** C256, 3118.
15. Lamprecht, G.; Hanus, D. *Neues Jahrb. Mineral Monatsh.* **1973,** 236.
16. Rahlfs, P. *Z. Phys. Chem. B.* **1936,** 31, 157.
17. Weller, W. W.; Kelley, K. K. *U.S. Bureau of Mines Rept. Inv. 6511,* **1964.**
18. Cemic, L.; Kleppa, O. J. *Geochim. Cosmochim. Acta* **1986,** 50, 1633.
19. Mehrotha, G. M.; Tare, V. B.; Wagner, J. B., Jr. *J. Electrochem. Soc.* **1985,** 132, 247.
20. Schaefer, S. C. *U.S. Bureau of Mines Rept. Inv. 8588,* **1981.**
21. Sharma, R. C.; Chang, Y. A. *Met. Trans.* **1980,** 11B, 139.
22. Deslatters, R. D.; Henins, A. *Phys. Rev. Lett.* **1973,** 31, 972.
23. Parise, J. B. *Acta Cryst.* **1980,** B36, 1179.
24. Fleet, M. E. *Am. Mineral.* **1977,** 62, 341.
25. Fleet, M. E. *Acta Cryst.* **1972,** B28, 1237.
26. Westrum, E. F., Jr.; Furukawa, G. T.; McCullough, J. P. *Experimental Thermodynamics, Vol. I.* McCullough, J. P.; Scott, D. W.: editors. Butterworths: London. **1968,** p. 133.
27. Grønvold, F. *Acta Chem. Scand.* **1967,** 21, 1695.
28. Mah, A. D.; Pankratz, L. B. *U.S. Bureau of Mines Bull. 668,* **1976.**
29. Pankratz, L. B.; Stuve, J. M.; Gokcen, N. A. *U.S. Bureau of Mines Bull. 677,* **1984.**
30. Grønvold, F.; Westrum, E. F., Jr. *J. Chem. Thermodynamics* **1986,** 18, 381.
31. Grønvold, F.; Westrum, E. F., Jr. *J. Chem. Thermodynamics* **1987,** 19, 1183.
32. Shaviv, R.; Westrum, E. F., Jr.; Grønvold, F.; Stølen, S.; Inaba, A.; Fuji, H.; Chihara, H. *J. Chem. Thermodynamics* **1989,** 21, 631.

33. Conde, C.; Manolikas, C.; Dyck, D. van; Delavignette, P.; Landuyt, J. van; Amelinckx, S. *Mater. Res. Bull.* **1978,** 13, 1055.
34. Dyck, D. van; Conde, C.; Amelinckx, S. *Phys. Stat. Sol.* **1979,** a56, 327.
35. Oliveira, M.; McMullan, R. K.; Wuensch, B. J. *Solid State Ionics* **1988,** 28–30, 1332.
36. Morimoto, N.; Kullerud, G. *Am. Mineral.* **1963,** 48, 110.
37. Gasymov, G. B.; Asadov, Yu. G.; Guseinov, G. G.; Gezalov, M. A.; Belov, N. V. *Dokl. Akad. Nauk SSSR* **1978,** 239, 846.
38. Anderson, J. S. *J. Chem. Soc. Dalton Trans.* **1973,** 1107.
39. Vallet, P.; Carel, C. *Rev. Chim. Mineral.* **1986,** 23, 362.
40. Black, S. N.; Jefferson, D. A.; Henderson, P. *J. Solid State Chem.* **1984,** 53, 76.
41. Strässler, S.; Kittel, C. *Phys. Rev.* **1965,** 139, A758.
42. Rice, M. J.; Strässler, S.; Toombs, G. A. *Phys. Rev. Lett.* **1974,** 32, 596.
43. Huberman, B. A. *Phys. Rev. Lett.* **1974,** 32, 1000.
44. Welsch, D. O.; Dienes, G. J. *J. Phys. Chem. Solids* **1977,** 38, 311.
45. Lam, L.; Bunde, A. *Z. Physik B* **1978,** 30, 65.